ELSEVIER

Tribology International 36 (2003) 205–212

TRIBOLOGY INTERNATIONAL

www.elsevier.com/locate/triboint

Thermoelastic instability in a thin layer sliding between two half-planes: transient behaviour

L. Afferrante, M. Ciavarella *, P. Decuzzi, G. Demelio

Centro di Eccellenza in Meccanica Computazionale (CEMEC), Politecnico di Bari, Viale Japigia 182, 70126–Bari, Italy

Received 8 March 2002; received in revised form 14 October 2002; accepted 18 October 2002

Abstract

The susceptibility of brakes and clutches to the known phenomenon of frictionally-excited thermoelastic instability is estimated studying the interface temperature and pressure evolution with time. A simple model has been considered where a layer with half-thickness a slides with speed V between two rigid and non-conducting half-planes. The advantage of this fairly simple model is that it permits us to deduce analytically the critical conditions for the onset of instability, that is the relation between the critical speed V_{cr} and the growth rate b of the interface temperature and pressure. It has then been verified that as the thickness a reduces the system becomes more and more prone to instability, and that a symmetrical pressure/temperature distribution at the layer interfaces can be more unstable than an antisymmetrical one. Moreover, the analysis of the evolution of the system beyond the critical conditions has shown that even if low frequency perturbations are associated with small critical speed, they might be less critical than high frequency perturbations if the working sliding speed is much larger than the actual critical speed of the system.

Keywords: Hot spotting; Thermoelastic instability; Brakes and clutches

1. Introduction

When two bodies are in sliding contact with relative speed V, the heat flux q generated at the interface is proportional to the contact pressure distribution p, that is to say $q=fVp$, where f is the frictional coefficient. Usually, the contact pressure p is not uniform because of surface waviness and roughness, geometric imperfections and mechanical vibrations. Consequently, the heat flux q is not uniform involving non-uniform thermal distortions of the contact interface, which, in turn, affect the contact pressure distribution p. This feedback between interface frictional heat and thermomechanical deformation can be unstable leading to the phenomenon known as frictionally-excited thermoelastic instability (TEI) ([1]). The occurrence of TEI in brakes and clutches might lead to the formation of hot spots, small regions where high temperature and pressure are experienced, which are responsible for an increase in wear rate, thermomechanical damage, vibrations, noise and thermal cracking ([2–5]).

Burton et al. [6] have proposed the first analytical model for estimating the occurrence of TEI, where two thermoelastic half-planes are considered in sliding contact along their common interface. The idea of a critical sliding speed V_{cr} was introduced: if the sliding speed V is larger than a critical value V_{cr}, which is a function of the material properties and geometry, the system is unstable. However, Burton's model overestimates somehow the critical speed because it does not consider the finite thickness of the brake or clutch disks. The effect of the thickness of the disks has been addressed in Lee and Barber [7] (L&B), who considered a model made up with a metallic layer sliding between two halfplanes of frictional material, which has been further refined by Decuzzi et al. [8] where frictional layers with finite thickness have been considered too. All the models listed above are dedicated to the estimation of the critical conditions for the onset of thermoelastic instability.

In this work, the evolution of the system with time is considered. The model analyzed is that of a metal layer sliding between two rigid and not conducting half-

* Corresponding author. Fax: +39-080-548-25-33.
E-mail address: m.ciavarella@area.ba.cnr.it (M. Ciavarella).

0301-679X/02/$ - see front matter © 2002 Elsevier Science Ltd. All rights reserved.
PII: S0301-679X(02)00185-8

Nomenclature

a	metal layer half-thickness [m]
b	growth rate [s^{-1}]
c	perturbation absolute speed [m/s]
c_i	perturbation relative speed with respect to the body i [m/s]
c_{p2}	specific heat of the metal layer [J/kg °C]
E	Young's modulus [N/m^2]
f	frictional coefficient
j	imaginary unit
k_2	diffusivity of the metal layer [m^2/s]
K_2	thermal conductivity of the metal layer [W/m °C]
m	wave number [m^{-1}]
p	contact pressure distribution [N/m^2]
q	heat flux [W/m^2]
q_{y2}	heat flux in metal layer [W/m^2]
T	temperature field [°C]
T_2	temperature field in metal layer [°C]
u_y	displacements at the sliding interface [m]
V	sliding speed [m/s]
V_{cr}	critical sliding speed [m/s]
α	thermal expansion coefficient [$°C^{-1}$]
λ	wave length [m]
μ	shear modulus [N/m^2]
ν	Poisson's coefficient
σ_{xy}	shear stresses at the sliding interface [N/m^2]
ρ_2	density of the metal layer [Kg/m^3]

planes, as introduced by Barber and Hector [9], in the following referred as to B&H.

2. Model and formulation

The model under analysis is made up of a thin metal layer (2) with thickness $2a$, representing the brake disk, and two rigid and not conducting half-planes (1) representing the brake pads, as shown in Fig. 1. The metal layer (2) has a relative speed V with respect to the two half-planes (1), and a uniform pressure p_0 is remotely applied to ensure complete contact along the interface. The formulation is similar to classical TEI work by Burton et al. [6] and Lee and Barber [7]. Although some of the analytical results are new, the expert reader may perhaps prefers to jump to the results section in Section 3.

The uniform contact pressure is perturbed superimposing a sinusoidal perturbation with wave number m at the sliding interface (y=0) having the form

$$p(x,t) = p_0 e^{bt} e^{jmx} \tag{1}$$

where b is the growth rate and j is the imaginary unit ($j^2=-1$). Following Burton et al. [6], the thermoelastic stability of the system is studied by means of a perturbation technique: the conditions under which the pertur-

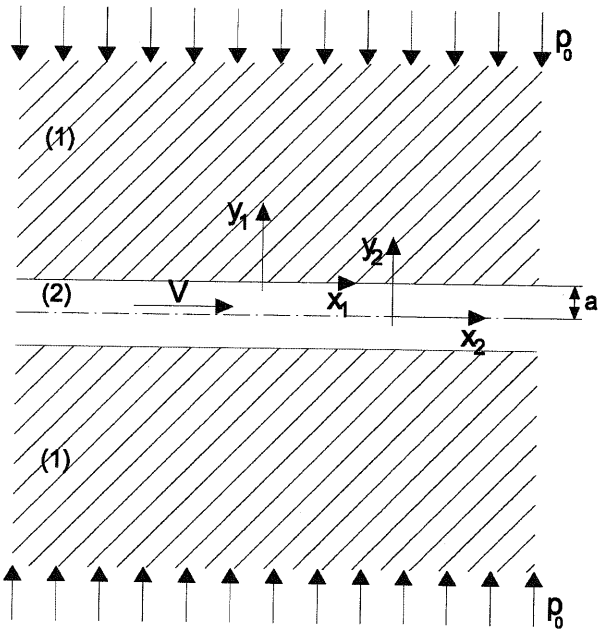

Fig. 1. A thin metal layer (2) sliding with relative speed V between two rigid not conducting half -planes (1).

bation can grow with time are examined. The perturbation has an absolute speed c along the x direction and relative speeds c_i with respect to the two bodies i (i=1,2). Since Burton et al. [6] have shown that the pressure perturbation is almost stationary with respect to the good conducting material, it derives that $c_2 \simeq 0$ and $c_1 = c = V$. Two frames of reference stationary with body (1) and (2) are introduced, as in Fig. 1, where $x = x_2 = x_1 - Vt$ and $y = y_1 = y_2 - a$.

The geometry of the system is symmetrical with respect to the middle-plane of the layer, but it does not imply a similar symmetry for the stress and temperature fields. Under the small perturbation hypothesis, the linearity of the problem is preserved, thus an arbitrary perturbation can be described as the superposition of symmetrical and antisymmetrical components. The perturbation with the highest growth rate b dominates over the others.

The frictional heat q_y generated at the sliding interface enters the sole conducting body (2), being the half-plane (1) an insulator, that is to say

$$q_y = q_{y2} = -K_2 \left.\frac{\partial T_2}{\partial y_2}\right|_{y=0} = fVp_0 e^{bt} e^{jmx}. \tag{2}$$

Further, the non uniform temperature distribution, solution of the heat conduction equation $k_2(\partial^2 T_2/\partial x_2^2 + \partial^2 T_2/\partial y_2^2) = \partial T_2/\partial t$, has the form $T_0 e^{bt} e^{jmx}$.

2.1. Symmetrical problem

From Lee and Barber [7], we know that, for a symmetrical problem, the temperature field in body (2) is given by

$$T_2(x,y,t) = \theta(y) e^{bt} e^{jmx} = T_0 \frac{\cosh[\lambda_2(y + a)]}{\cosh[\lambda_2 a]} e^{bt} e^{jmx} \tag{3}$$

where

$$\lambda_2 = \left(m^2 + \frac{b}{k_2}\right)^{1/2}. \tag{4}$$

Therefore, substituting Eq. (3) into (2), we obtain

$$(K_2 \lambda_2 \tanh[\lambda_2 a]) T_0 = fVp_0. \tag{5}$$

As shown in Barber and Hector [9], since the frictional pads are non-conducting the temperature field is exclusively perturbed in the metal layer. Further, since they are also rigid, the displacements u_y and the stresses σ_{xy} at the sliding interface are zero. It may be shown that the temperature perturbation $T_2(x, y, t)$ causes a pressure distribution on the sliding interface expressible as $p(x, t) = p_0 e^{bt} \cos(mx)$, with

$$p_0 = \frac{8\beta\mu m}{(\kappa + 1)\sinh[2ma]} \int_{-a}^{+a} \cosh[m(s_2 \pm a)]\theta(s_2) ds_2 \tag{6}$$

where $\mu = E/[2(1 + \nu)]$ is the shear modulus and

$$\beta = \alpha \quad \text{for plane stress} \qquad = \alpha(1 + \nu) \quad \text{for plane strain} \tag{7}$$

$$\kappa = \frac{3-\nu}{1+\nu} \quad \text{for plane stress} \qquad = 3 + 4\nu \quad \text{for plane strain.} \tag{8}$$

The choice of the sign + or −, in Eq. (6), is indifferent. Rephrasing the above formula with respect to the frame of reference fixed on the sliding interface,

$$p_0 = \frac{8\beta\mu m}{(\kappa + 1)\sinh[2ma]} \int_{-2a}^{0} \cosh[m(s + 2a)]\theta(s) ds. \tag{9}$$

Substituting for $\theta(y)$, as from (3), in (9), integrating and rearranging, it results in

$$p_0 = \frac{8\beta\mu m T_0}{(\kappa + 1)} \left(\frac{\lambda_2 \coth[ma]\tanh[\lambda_2 a] - m}{\lambda_2^2 - m^2}\right). \tag{10}$$

From Eq. (5) with the above result, there follows the following characteristic equation

$$K_2 \lambda_2 \tanh[\lambda_2 a] = fV \frac{8\beta\mu m}{(\kappa + 1)} \left(\frac{\lambda_2 \coth[ma]\tanh[\lambda_2 a] - m}{\lambda_2^2 - m^2}\right). \tag{11}$$

For fixed material and geometrical properties, Eq. (11) gives the dependence of the sliding speed V on the growth rate b, being λ_2 a function of b as from (4). Under plane strain assumption, Eq. (11) becomes

$$\lambda_2 \tanh[\lambda_2 a] = \frac{fV}{k_2} \tilde{H}_2 \left(\frac{\lambda_2 \coth[ma]\tanh[\lambda_2 a] - m}{\lambda_2^2 - m^2}\right) \tag{12}$$

where

$$\tilde{H}_2 = \frac{2a(1 + \nu)\mu k_2}{K_2(1-\nu)}. \tag{13}$$

Considering the expression for λ_2, as from (4), after some algebra, it follows that

$$\tilde{H}_2 = \frac{2a(1 + \nu)\mu k_2}{K_2(1-\nu)}. \tag{13}$$

from which the critical speed can be readily determined for $b \to 0$

$$V_{cr} = \frac{4k_2}{f\tilde{H}_2} \frac{m\sinh^2[ma]}{2ma + \sinh[2ma]}. \tag{15}$$

Unstable perturbations have $b > 0$.

2.2. Antisymmetrical problem

From Lee and Barber [7], we know that for the antisymmetrical problem the temperature field in body (2) is given by

$$T_2(x,y,t) = \theta(y)e^{bt}e^{jmx} = T_0\frac{\sinh[\lambda_2(y+a)]}{\sinh[\lambda_2 a]}e^{bt}e^{jmx} \quad (16)$$

while, from (9) the contact pressure is given by

$$p_0 = \frac{8\beta\mu m T_0}{\kappa+1}\left(\frac{\lambda_2\tanh[ma]\coth[\lambda_2 a]-m}{\lambda_2^2-m^2}\right). \quad (17)$$

Finally, the characteristic equation is obtained substituting (16) and (17) into (2):

$$K_2\lambda_2\coth[\lambda_2 a] = fV\frac{8\beta\mu m}{(\kappa+1)}\left(\frac{\lambda_2\tanh[ma]\coth[\lambda_2 a]-m}{\lambda_2^2-m^2}\right). \quad (18)$$

Therefore, for the antisymmetrical problem, the dependence of the sliding speed on the growth rate is

$$V = -\frac{b\sqrt{m^2+\frac{b}{k_2}}\coth\left[a\sqrt{m^2+\frac{b}{\kappa_2}}\right]}{f\tilde{H}_2 m\tanh[ma]\sqrt{m^2+\frac{b}{k_2}}\coth\left[a\sqrt{m^2+\frac{b}{k_2}}\right]-f\tilde{H}_2 m^2} = 0 \quad (19)$$

from which the critical speed can be readily determined for $b\to 0$,

$$V_{cr} = \frac{4k_2}{f\tilde{H}_2}\frac{m\cosh^2[ma]}{\sinh[2ma]-2ma}. \quad (20)$$

2.3. Dimensionless formulation

Introducing the dimensionless parameters

$$\tilde{b} = \frac{b}{m^2k_2};\ \tilde{V} = \frac{V}{mk_2} \quad (21)$$

the dependence of the dimensionless sliding speed on the dimensionless growth rate, for symmetrical (Eq. (22)) and antisymmetrical (Eq. (23)) conditions, becomes, respectively

$$\tilde{V}_{sym} = \frac{1}{f\tilde{H}_2}\frac{\tilde{b}\sqrt{1+\tilde{b}}\tanh[ma\sqrt{1+\tilde{b}}]}{\coth[ma]\sqrt{1+\tilde{b}}\tanh[ma\sqrt{1+\tilde{b}}]-1} \quad (22)$$

$$\tilde{V}_{asym} = \frac{1}{f\tilde{H}_2}\frac{\tilde{b}\sqrt{1+\tilde{b}}\coth[ma\sqrt{1+\tilde{b}}]}{\tanh[ma]\sqrt{1+\tilde{b}}\coth[ma\sqrt{1+\tilde{b}}]-1}. \quad (23)$$

Consequently the dimensionless sliding speed assumes the following forms:

$$\tilde{V}_{cr\,sym} = \left(\frac{V_{cr}}{mk_2}\right)_{sym} = \frac{4}{f\tilde{H}_2}\frac{\sinh^2[ma]}{2ma+\sinh[2ma]}, \quad (24)$$

$$\tilde{V}_{cr\,asym} = \left(\frac{V_{cr}}{mk_2}\right)_{asym} = \frac{4}{f\tilde{H}_2}\frac{\cosh^2[ma]}{\sinh[2ma]-2ma}. \quad (25)$$

3. Results

In the following paragraphs, the behaviour of the growth rate b with the sliding speed is presented as a function of the layer thickness and the wave number m, together with the critical sliding speed. In addition, the interface temperature distribution T is given as a function of time.

The material properties of the metal layer are those commonly used for cast iron disks in automotive applications, as reported in the Table 1.

3.1. Comparison between the symmetrical and antisymmetrical sliding speed

In Fig. 2 the dependence of the dimensionless critical speed $\tilde{V}_{cr} = V_{cr}/mk_2$ on the wave parameter ma is shown for both symmetrical and antisymmetrical boundary conditions, as given in Eqs (24) and (25). It appears that the critical speed for the symmetrical case is lower than the speed for the antisymmetrical case, thus the former is more critical than the latter. For ma going to ∞, both cases tend to the known Burton's solution ($\tilde{V}_{cr\,Burton} = (V_{cr}/mk_2)_{Burton} = 2/f\tilde{H}_2$) which has been deduced for half-planes model ($a\to\infty$). The above result is apparently in contrast with what has been found by Lee and Barber [7], who showed the antisymmetrical condition to be more critical than the symmetrical case for a set of material properties commonly used in automotive applications (Fig. 3: lines with L&B). In the present solution, rigid frictional half-planes ($E_1\to\infty$) are considered, and this explains the above observations. For a practical braking system, the thermal conductivity of the frictional material is small compared to that of the metal disk. Thus the assumption of non-conducting material has no substantial influence on the results. In fact, for symmetrical conditions, as the thickness a decreases, it is more and more 'difficult' to squeeze the metal layer between the rigid half-planes: the pressure perturbation and the surface thermal displacements are in phase concordance on the opposite faces of the layer, and the critical speed drops to zero for $ma=0$. Conversely, for antisymmetrical conditions, as the thickness a decreases it is easier to 'bend' the layer: the pressure perturbation and the surface thermal displacements are in phase opposition on the opposite faces of the layer, and the critical speed goes to infinity for $ma=0$.

In addition, Fig. 3 shows the behaviour of the critical speed for the case in which the metal layer and the half-planes have identical elastic moduli $E_1=E_2$. It is fairly clear how the symmetric curve tends to be more critical than the antisymmetric one. It can be expected that for some applications where the frictional pad is sufficiently stiff to reduce wear the most critical condition would be that of a symmetrically deforming layer.

The following discussion is limited to the symmetrical

Table 1
Characteristic values of the physical constants for the metal layer

Material	$E\left(\frac{N}{m^2}\times 10^9\right)$	ν	$\alpha(°C^{-1}\times 10^{-6})$	$K\left(\frac{W}{m°C}\right)$	$k\left(\frac{m^2}{s}\times 10^{-6}\right)$
Cast iron	125	0.25	12	54	12.98

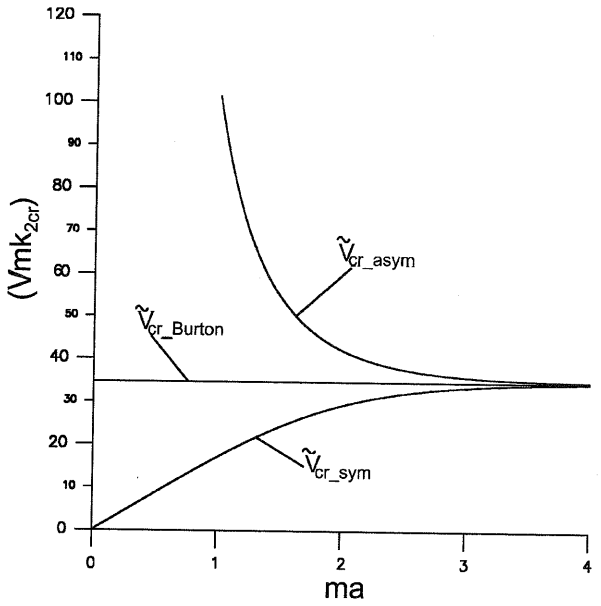

Fig. 2. A comparison between the dimensionless critical speeds for the symmetrical and asymmetrical mode and the Burton's solution as a function of the wave parameter *ma*.

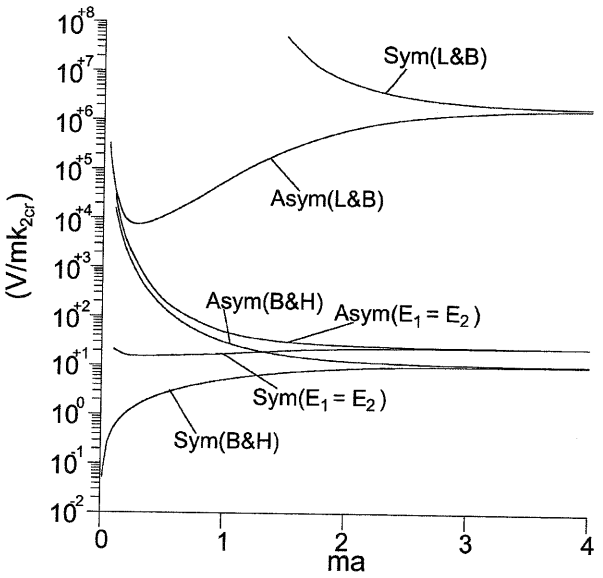

Fig. 3. A comparison between the symmetrical and asymmetrical critical speeds for the (i) Lee and Barber material set (L&B), (ii) the present material set (B&H) and (iii) the case of materials with identical elastic moduli (E_1=E_2).

case, which is the dominant mode for the present problem.

3.2. The growth rate b

In order to get the growth rate b as a function of the sliding speed V, the relation (14) has to be inverted numerically. In Fig. 4, the curves $b(V)$ are shown for different values of the wave number m, namely m=200, 500 [m^{-1}], and for a=0.005 [m] and a=0.05 [m]. The critical speed in Fig. 4 is determined by the intersection of the curve $b(V)$ at the horizontal axes (b=0). It appears that for a fixed layer thickness, as the wave number m is increased the critical speed increases: longer waves are more critical than shorter. However, it can also be observed that, at fixed thickness, curves with different wave numbers intersect each other, meaning that shorter waves (higher m) can dominate for sufficiently large sliding speeds on the longer waves (lower m).

Moreover, at fixed wave number, as the thickness of the layer increases the critical speed increases whilst the growth rate for a fixed speed reduces: the system becomes more stable with growing a.

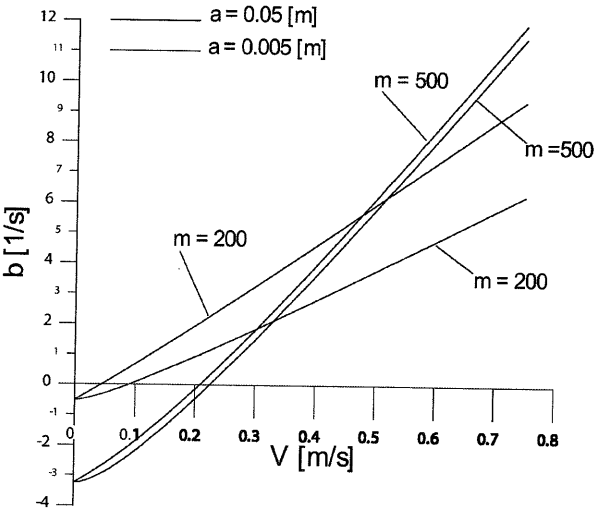

Fig. 4. The relation between the growth rate b and the sliding speed V (Eq. (14)), for two different values of the wave number (m=200, 500 [m^{-1}]) and thickness (a=0.005, 0.05 [m]).

In Fig. 5, the dimensionless sliding speed is plotted against the dimensionless growth rate for different values of the wave parameter *ma*, with $f\tilde{H}_2 = 0.0577$. As the wave parameter *ma* reduces at fixed speed the growth rate b increases, and as from Fig. 4, higher wave parameters *ma* lead to higher critical speeds. Again, as *ma* goes to infinity, the Burton's solution is approached.

3.3. Transient evolution of the temperature field

As shown in Al-Shabibi and Barber [10], a general solution for the transient evolution of a perturbation at constant sliding speed can be written as an eigenfunction series

$$T(x,y,z,t) = \sum_{i=1}^{n} C_i e^{b_i t}\theta_i(x,y,z) \tag{26}$$

where n is the number of eigenfunctions and C_i is a set of arbitrary constants determined from the initial condition $T(x, y, z, 0)$. The term with the largest value of $\mathrm{Re}[b_i]$ will dominate the transient response, so it is the only term which needs to be considered. Thus,

$$\frac{\partial T}{\partial t} = be^{bt}\theta_1 - bT \tag{27}$$

where b is the growth rate of the term which dominates the transient regime. These results apply only if contact is maintained at all times and the sliding speed V is constant. However, an approximate solution to the problem with variable speed can be defined by considering b as the dominant growth rate at the instantaneous speed $V(t)$.

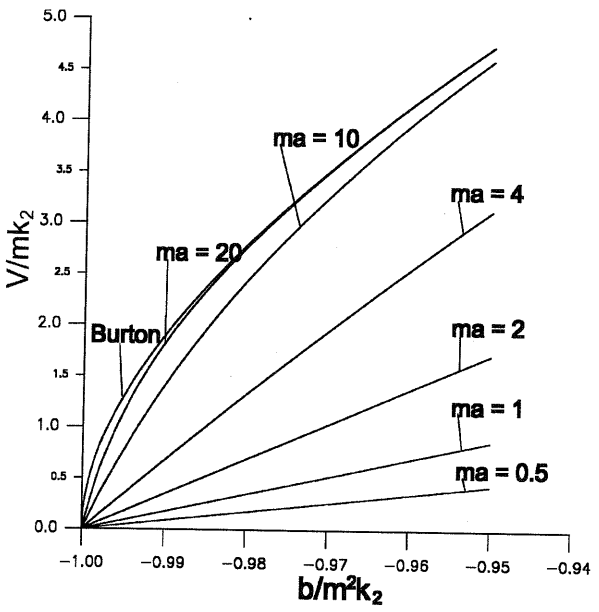

Fig. 5. Variation of the dimensionless growth rate b with the sliding speed V as the wave parameter *ma* increases: the Burton's solution is sufficiently accurate for *ma* about 20.

Therefore the pressure and temperature fields in the transient regime can be written as

$$T = T(0)\exp\{\int_0^t b(v(t))\mathrm{d}t\} \tag{28}$$

$$p = p(0)\exp\{\int_0^t b(v(t))\mathrm{d}t\} \tag{29}$$

where $T(0)$ and $p(0)$ are the temperature and contact pressure at the time t=0, and $b(t)$ is intended as the dominant growth rate at each speed $V(t)$.

From (14), $V(t)$ is expressed as a function of b. But the relation cannot be inverted analytically. However, assuming a linear variation of the sliding speed V with time t

$$V(t) = V_0\left(1 - \frac{t}{t_0}\right) \tag{30}$$

with V_0 and t_0 the initial sliding speed and stopping time, respectively, it can be derived:

$$\bar{\tau} = \frac{t}{t_0} = 1 - \frac{1}{f\tilde{H}_2 V_0}\, b\sqrt{m^2 + \frac{b}{k_2}}\tanh\left[a\sqrt{m^2 + \frac{b}{k_2}}\right] m\coth[ma]\sqrt{m^2 + \frac{b}{k_2}}\tanh\left[a\sqrt{m^2 + \frac{b}{k_2}}\right] = m^2 \tag{31}$$

Placing $\bar{\tau} = b^{-1}(b)$, it results:

$$\int_0^{\bar{\tau}_1} b(\bar{\tau})\mathrm{d}\bar{\tau} = \int_{b(\bar{\tau}=0)}^{b(\bar{\tau}=\bar{\tau}_1)} b(b^{-1}(b))\frac{\mathrm{d}b^{-1}(b)}{\mathrm{d}b}\mathrm{d}b = \int_{b(\bar{\tau}=0)}^{b(\bar{\tau}=\bar{\tau}_1)} b\frac{\mathrm{d}\bar{\tau}}{\mathrm{d}b}\mathrm{d}b \tag{32}$$

where $\bar{\tau}_i$ is a dimensionless time instant in the evolution of the process and $b(\bar{\tau}_i)$ is derived from (31). Therefore the integrals in (28) and (29) take the form

$$\frac{T}{T(0)} = \exp\left\{\int_{b(\bar{\tau}=0)}^{b(\bar{\tau}=\bar{\tau}_i)} b\frac{\mathrm{d}\bar{\tau}}{\mathrm{d}b}\mathrm{d}b\right\} \quad \text{for } i = 1, 2, \ldots, n \tag{33}$$

$$\frac{p}{p(0)} = \exp\left\{\int_{b(\bar{\tau}=0)}^{b(\bar{\tau}=\bar{\tau}_i)} b\frac{\mathrm{d}\bar{\tau}}{\mathrm{d}b}\mathrm{d}b\right\}, \tag{34}$$

where n is the number of time instants in which to estimate the temperature.

In Fig. 6, the transient evolution of the temperature distribution is presented for different values of m, as from Eq. (33), for a cast iron disk, and V_0=0.8 [m/sec], a=0.005 [m]. The temperature amplitude grows from $T(0)$, reaches a maximum and then reduces with time. The maximum value and position (time) is a function of m. All the perturbations with a wave number larger than $m \geq 1778$ [m^{-1}] are stable with T decreasing with time. For such value, in fact, the sliding speed is always maintained under the critical value. Furthermore, the long waves are more critical than short waves for values of the wave number $m \leq 400$ [m^{-1}]. Above this limit the situation is reversed, that is the perturbations with greater wave length become less "harmful" for the system.

In Fig. 7, the maximum of the temperature field T_{max}, normalized with respect to its initial value $T(0)$, is plotted as a function of the wave number m. For sort values of m, such maximum grows with the wave number. Vice versa, for m>400 [m^{-1}] , the increase of the wave number involves a reduction of T_{max}. Therefore, the perturbation with m=400 [m^{-1}] is the most critical perturbation for the system, because it dominates over the others. However, it must be noticed that the finite circular extension of disks in a braking system imposes a limit on the minimum supportable wave number as observed in Lee and Barber [7]. In fact, between the wave number m and the mean radius of the disk R_m, exists the following relation: $m=N/R_m$, where N is the number of hot spots. For example, if R_m=0.05 [m] is considered as the mean radius, for N=1 it is possible to derive the perturbation with the shorter wave number (m=20 [m^{-1}]) compatible with the physical size of the disk. Clearly, perturbations with $m \leq 20$ [m^{-1}] must not be considered in this example.

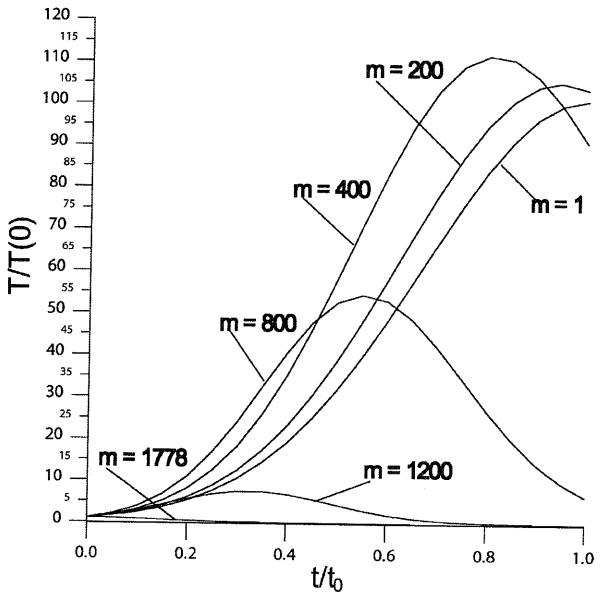

Fig. 6. Transient evolution of the temperature perturbation, normalized with respect to its initial value $T(0)$, for different values of the wave number m (a=0.005 [m]).

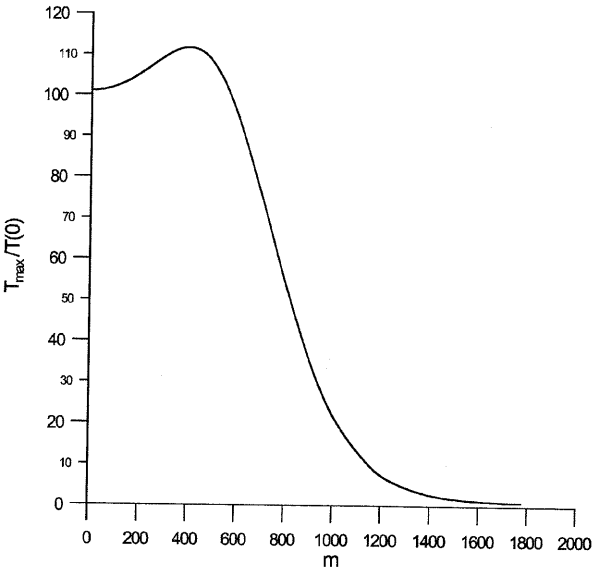

Fig. 7. Variation with wave number m of the maximum of the temperature perturbation, normalized with respect to its initial value $T(0)$ (a=0.005 [m]).

3.3.1. Dimensionless formulation

Introducing the dimensionless time

$$\tau = k_2 m^2 t \tag{35}$$

and recalling (21), (31) can be rewritten as

$$\frac{\tau}{\tau_0} = 1 - \frac{1}{f\tilde{H}_2\tilde{V}_0} \frac{\tilde{b}\sqrt{1+\tilde{b}}\tanh[ma\sqrt{1+\tilde{b}}]}{\coth[ma]\sqrt{1+\tilde{b}}\tanh[ma\sqrt{1+\tilde{b}}]-1} \tag{36}$$

Therefore, keeping in mind (32), the temperature perturbation becomes

$$\frac{T}{T(0)} = \exp\left\{ \int_{\tilde{b}(\tau=0)}^{\tilde{b}(\tau=\tau_i)} \tilde{b}\frac{d\tau}{d\tilde{b}} d\tilde{b} \right\} \quad \text{for } i = 1, 2, \ldots, n. \tag{37}$$

In Fig. 8, the relation between Y/T (0) and τ is presented for different values of the dimensionless wave number ma, namely: ma=2; ma=2.5; ma=3; ma=3.5, with $f\tilde{H}_2\tilde{V}_0 = 10$ and τ_0=3.82. It is evident that Burton's model for small thicknesses of the disk underestimates the growth of the temperature and pressure perturbation, whilst it is sufficiently accurate for large ma.

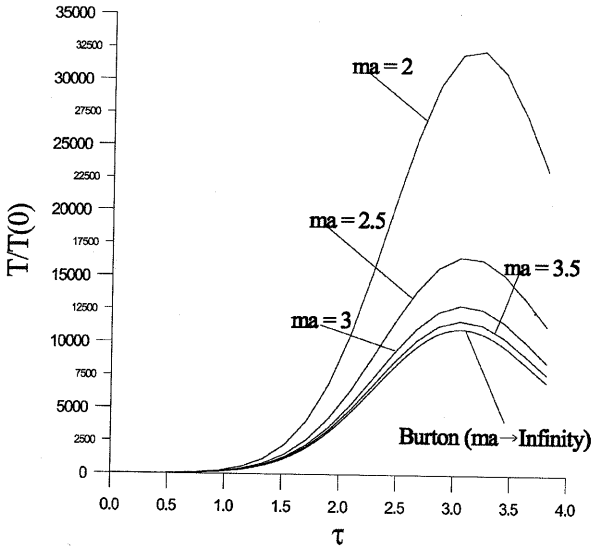

Fig. 8. Evolution with dimensionless time (τ=km^{2}t) of the temperature perturbation, normalized with respect to its initial value $T(0)$, for different values of the wave parameter *ma*.

4. Conclusions

The model of an elastic layer sliding between two rigid half-planes has been studied with reference to thermoelastic instability. The model is somehow arbitrary in reproducing the correct thermoelastic behaviour of brakes and clutches when the layer, representing the metal disk, is more rigid than frictional pads. However, the present model is close to the identical moduli case (E_1=E_2) which is typical of traditional tread brakes where both the pad and the disk are made up of cast iron. On the contrary, the limiting assumption of non-conducting pads is reasonable, since the thermal conductivity of the metal disk is much larger than that of the frictional material. However, the advantage of the present formulation with respect to that of Lee and Barber [7] (where both layer and half-planes are conducting and elastic) is that the heat flux is stationary with respect to the layer (c_2=0), permitting us to determine in closed form the relation between V_{cr} and b, and to study the transient evolution of the sliding system.

The following results can be summarized:

1. the Burton's solution (the half-plane model) is accurate only for sufficiently large wave parameters, namely $ma \geq 20$, and as the wave parameter grows the symmetrical and antisymmetrical modes tend to the same solution which is that given by Burton;
2. as the thickness a of the layer reduces, the critical speed V_{cr} decreases and the growth rate b increases, thus leading to a system which is more prone to thermoelastic instability;
3. low frequency perturbations have lower critical speed V_{cr} than high frequency perturbations, however the growth rate b of the high frequency perturbations increases with speed much faster than for the low frequency perturbations. Consequently, it is likely that for sufficiently large operating speeds, well above the critical speed, high frequency perturbations would dominate low frequency perturbations;
4. symmetrical conditions on the thin layer are more critical than antisymmetrical conditions, and such a behaviour has been verified also for frictional pads with sufficiently large elastic modulus, which is the case of applications where the wear of frictional materials is a major concern.

Acknowledgements

The authors wish to acknowledge Professor James R. Barber of the University of Michigan for his helpful comments.

References

[1] Barber JR. Thermoelastic instabilities in the sliding of conforming solids. Proc R Soc London 1969;A312:381–94.
[2] Anderson AE, Knapp RA. Hot spotting in automotive friction systems. Wear 1990;135:319–37.
[3] Takezaki K, Kubota M. Thermal and mechanical damage of paper wet friction material induced by non-uniform contact. SAE922095, 1992.
[4] Kreitlow W, Schrödter F, Matthtii H. Vibration and 'hum' of disk brakes under load. SAE850079, 1985.
[5] Lee K, Diwiddie RB. Conditions of frictional contact in disk brakes and their effects on brake judder. SAE 980598, 1998.
[6] Burton RA, Nerlikar V, Kilaparti SR. Thermoelastic instability in a seal-like configuration. Wear 1973;24:189–98.
[7] Lee K, Barber JR. Frictionally-excited thermoelastic instability in automotive disk brakes. ASME J Tribology 1993;115:607–14.
[8] Decuzzi P, Ciavarella M, Monno G. Frictionally excited thermoelastic multi-disk clutches and brakes. ASME J Tribology 2001;123:865–71.
[9] Barber JR, Hector LG. Thermoelastic contact problems for the layer. ASME J Appl Mech 1999;66:806–9.
[10] Al-Shabibi AM, Barber JR. Transient Solution of a two-dimensional TEI problem using a reduced order model. Int J of Mech Sc 2002;44:451–64.